



Photoluminescence and quenching in polyaniline/ZnS nanocomposites

Jayasudha Sriram¹, Ramya¹, Sreeja K. V.¹, Priya L.^{2*} and K. T. Vasudevan³

¹Dept. of Physics, CPGS, Jain University, Jayanagar 3rd Block, Bangalore-560011

²Department of Physics, LRG Government College for women, Tirupur – 641604

³Department of Physics, T. John College, 86/1, Gottigere, Bangalore - 560 083

ABSTRACT

Nanocomposites of conducting polyaniline with ZnS nanoparticles (PAni/ZnS) have been synthesized by in-situ polymerization of aniline monomer using ammonium persulphate as oxidizing agent. The weight percentage of ZnS is varied from 1% to 28%. The formation of PAni/ZnS composites was assessed by X-Ray Diffraction (XRD), Field Emission Scanning Electron Microscope (FESEM) and UV-Vis spectroscopy. The broadening sharp peaks in the XRD patterns indicated the formation of nanocrystalline phase of ZnS with crystallite size of ~5.3 nm. The FESEM image shows a nanoparticulate structure of ZnS and it is also seen that the ZnS nanoparticles are well dispersed in the polyaniline matrix. UV-Vis spectrum of composites shows two peaks at 340 nm and a broad peak in the range ~580 nm to 790 nm. The peak around ~340 nm corresponds to excitation of electron from valence to conduction band, is used to determine the nature and value of the optical band gap of composites. Photoluminescence studies were carried out by exciting the samples with an excitation wavelength of 320 nm. Two peaks are observed at a wavelength of ~365 nm and 520 nm. The 365 nm emission is due to recombination of electrons at the sulphur vacancy donor level with holes trapped at the zinc acceptor level. The Peak at ~520 nm with less intensity could be due to some self-activated defect centres related to Zn vacancies. Thermal stability of the sample was analysed by Differential Scanning Calorimetry. DSC thermogram shows 2 endothermic peaks at 125° C and 260 °C. DC conductivity of PAni and its composites have been measured in the temperature range from 25°C to 205°C. It is found that conductivity increases with the increase of ZnS concentration.

Key words: Quenching, photoluminescence, Differential Scanning Calorimetry, Polyaniline

INTRODUCTION

Polymer nanocomposites are the materials in which nanoscale inorganic particles are dispersed in an organic polymer matrix. When these particles are impregnated into a polymer matrix it enhances the stability of polymer while retaining its processing flexibility [1 – 5]. Polymeric nanomaterials are multicomponent system, where the primary component is polymer. Filler in these multicomponent systems is of lesser quantity and has at least one of the dimensions below 100 nm [6]. The properties of nanocomposite materials depend not only on the properties of the individual components but also on the microstructure and interfacial characteristics [7]. In some nanocomposites the predominant properties are due to interfacial interactions and in others property enhancements are mostly due to the quantum effects associated with nano dimensional structures [8]. Conjugated polymers are suitable for the formation of large area devices, and their energy gap and ionization potential can be tuned by chemical modification in the polymer chain. Conjugated polymer/ nanocrystal composites can be used for photovoltaic devices as charge separation. Charge separation in conjugated polymers has been found to be enhanced when the material at the interface is a material of higher electron affinity, which is energetically favourable for the electron to transfer [9]. Among the conjugated polymers Polyaniline (PAni) has got much importance due to its unique electrical, electrochemical properties, high environmental stability, easy polarization and low cost of monomer [10]. Since the conductivity of PAni depends on both the oxidation states of the main polymer chain as well as the degree of

protonation of the imine sites [11]. Any interaction with PANi that alters either of these processes will affect its conductivity. Polyaniline/inorganic particle nanocomposites have been studied for applications like electro-rheological fluids and in high density information storage devices [12].

Zinc sulphide (ZnS) an II-VI compound semiconductor is a very promising material for wide applications in electroluminescent and optoelectronic devices. The introduction of surface states with miniaturization of sample size affect the electronic energy states of wide band gap semiconductor. The optical properties of ZnS nanoparticles can be tuned by passivating surfaces with different organic molecules [13]. Luminescence measurements are one of the most important techniques to reveal the energy structure and surface state of these particles [14] and in determining the luminescence characteristics of the ZnS quantum dots [15]. It is reported that PANi shows photoluminescence indicating existence of multiple electronic states including polaron bands, defect bands and conduction bands [16]. Composite of PANi with ZnS had six times higher conductivity than pure PANi. The enhancement is due to the interfacial interaction with ZnS matrix and enhancement in the crystallinity [17, 18].

In the present work the structural, optical, thermal and electrical characteristics of PANi/ZnS nanocomposites are studied by varying the concentration of ZnS in PANi.

MATERIALS AND METHODS

Nanoparticles of ZnS were prepared by chemical co-precipitation method. All the chemicals were of AR grade and were used without further purification. Freshly prepared aqueous solutions of the chemicals were used for the synthesis of nanoparticles. ZnS nanoparticles were prepared at room temperature by dropping simultaneously 0.4M Zinc Sulphate solution and 0.5M Sodium Sulphide solution dissolved in distilled water containing 0.1M EDTA solution. It was vigorously stirred using magnetic stirrer. The role of EDTA is to stabilize the particles against aggregation. The prepared reaction mixture was kept for stirring for two hours at constant rate of stirring. The mixture was then left overnight. The precipitate was then separated from the reaction mixture, washed twice with distilled water to remove the impurities. The wet precipitate was dried and thoroughly grinded to get fine powder. The yield was calculated.

Polyaniline is prepared by dropping, 2M of APS dissolved in 500ml of 3M HCl to aniline dissolved in 500ml of 3M HCl with continuous stirring at 2°C. A dark green colour was seen indicating the formation of polyaniline. ZnS in PANi is obtained by mixing freshly prepared ZnS precipitate in PANi solution. The stirring was continued for 48 hours, so that the particles are completely dispersed into the PANi solution. The solution was then dialyzed against distilled water for 48 hrs to remove unreacted oxidants and other impurities. The final solution was poured into a Petri dish and kept for drying at room temperature. Dried samples were grinded to get fine powder. Nanocomposites of various wt% of ZnS in PANi (3%-PZ3, 5%-PZ5, 10%-PZ10 and 28%-PZ28) were prepared by a similar procedure.

CHARACTERIZATION TECHNIQUE

The phase and structure of the nanocomposites were studied in a Bruker X ray diffractometer using CuK_α radiation. The size and morphology of the ZnS nanoparticles were observed by FESEM in NEON 40 cross beam Carl Zeiss instrument. Optical absorption was measured in Shimadzu 1800 UV – Vis spectrophotometer. Room temperature photoluminescence (PL) of the samples were measured using JY Fluorolog-3-11 Spectrofluorometer. DC conductivity was measured using two probe setup. Differential Scanning Calorimetry is carried out in Mettler-Toledo DSC 1 instrument.

RESULTS AND DISCUSSION

X-RAY DIFFRACTION

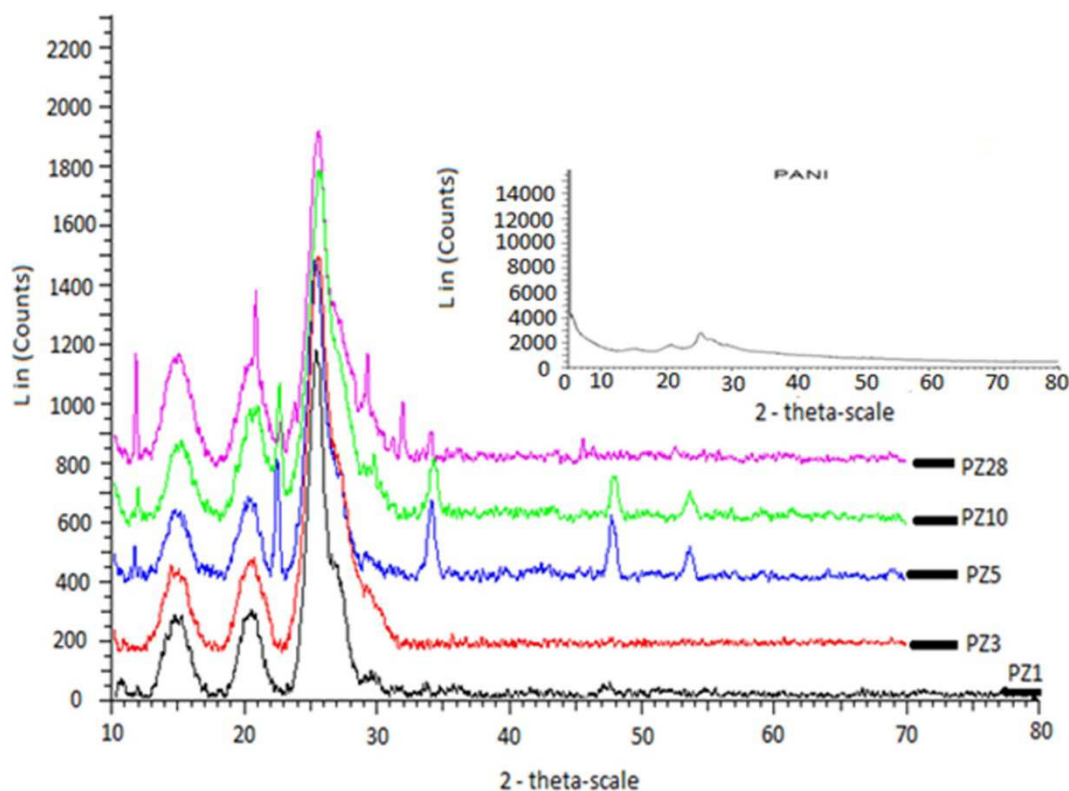


Figure 1: XRD pattern of the PANi / ZnS nanocomposites and PANi in the inset

XRD pattern of pure PANi, PANi/ZnS nanocomposites are shown in figure 1. The XRD pattern of PANi shows peaks around 20° and 25° with (111) and (110) plane respectively [19]. In the nanocomposites there are four prominent peaks at 26° , 34° , 48° and 53.5° corresponding to hexagonal wurtzite phase of ZnS [JCPDS No.36-1451]. There is an obvious broadening of the XRD pattern which indicates the formation of nano sized ZnS. A single broad peak at 26° is obtained in the scan range $2\theta=23^\circ-32^\circ$ which is the result of the overlap of three wurtzite peaks (100), (002) and (101), at 2θ positions 26.91° , 28.49° and 30.54° respectively [20, 21].

The benzenoid and quinonoid units are more orderly arranged in PANi/ZnS nanocomposites compared to pure PANi. The low intensity peak at 11° indicates that the PANi has amorphous nature. The peak at 15° indicates that the nanoparticles promote the formation (010) plane of PANi during the polymerization process [22, 23]. It is observed that Peaks at 34° , 48° and 53.5° shifts to the lower 2θ value as the concentration of ZnS increases. The degree of crystallinity is increased in PANi/ZnS nanocomposites with increasing concentration of ZnS compared to pure PANi, indicating the homogeneous distribution of nanoparticles in the polymer matrix. The size of ZnS nanoparticles was determined from the full width at half maxima (FWHM) of the peaks, using Scherrer formula. The average particle size of PANi/ZnS is found to be 5.3 nm.

FESEM

FESEM images of PANi, ZnS, PZ5 and PZ28 are shown in figure 2. It is an efficient tool to determine nano dispersion in the polymer matrix. It is found that the ZnS nanoparticles are well dispersed in PANi and are spherical. The FESEM image confirms the formation of hybrid material of PANi/ZnS nanocomposites. PANi is seen as an interconnected region. This supports the fact that, ZnS particles had a nucleation effect on the PANi [18]. The presence of spherical ZnS can be seen very clearly in PANi/28% ZnS compared to 5%. A good dispersion of nanoparticles in the polymer matrix is seen in the images which are necessary to achieve an enhancement in optical and electrical properties.

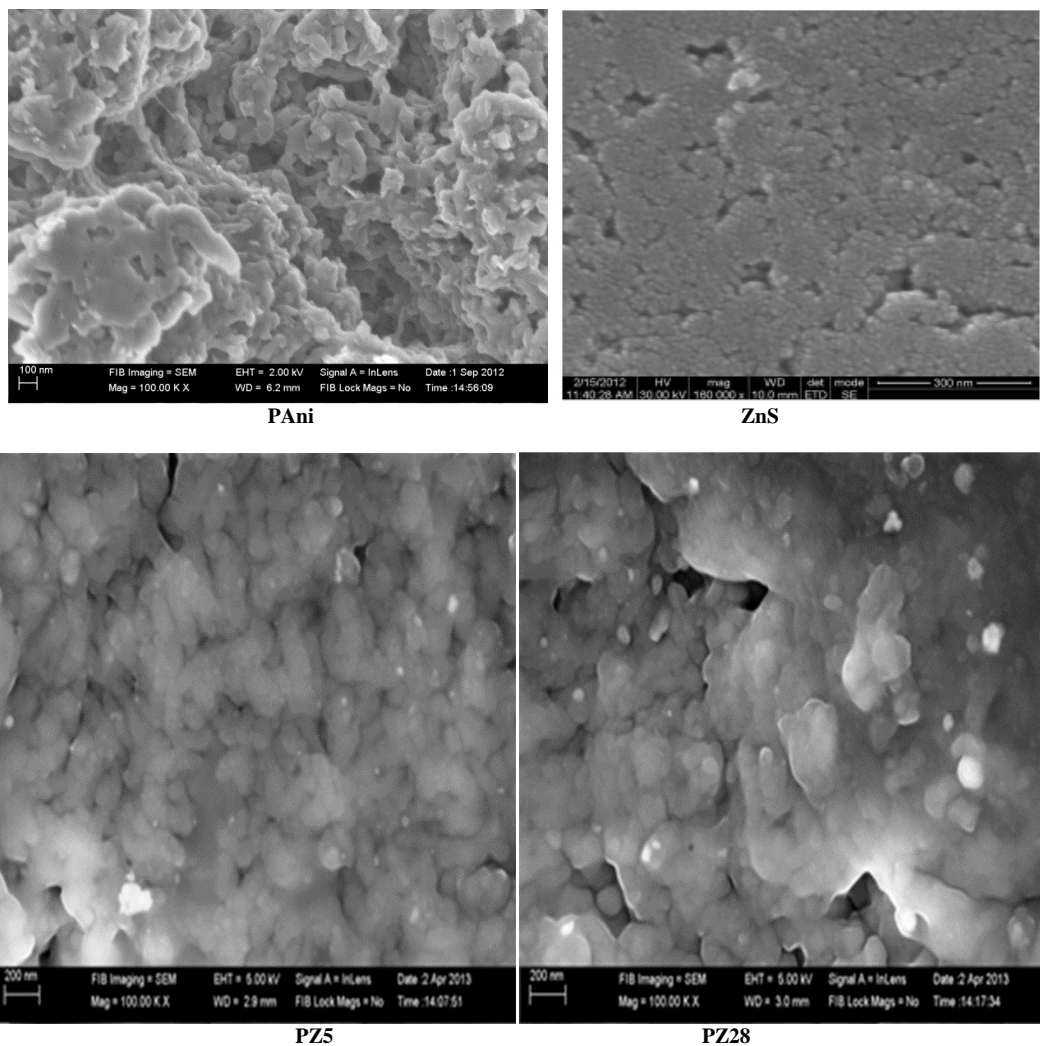


Figure 2. SEM images of PAni, ZnS, PZ5 and PZ28

UV-Vis Spectroscopy

UV-Vis absorption characteristics of the samples are shown in figure3. The UV-Vis spectra of ZnS nanoparticles consist of a peak around 325 nm which corresponds to a band gap of 3.4 eV. A strong absorption peak found around 325 nm is blue Shifted compared to the absorption peak of the bulk ZnS (345 nm) [24].

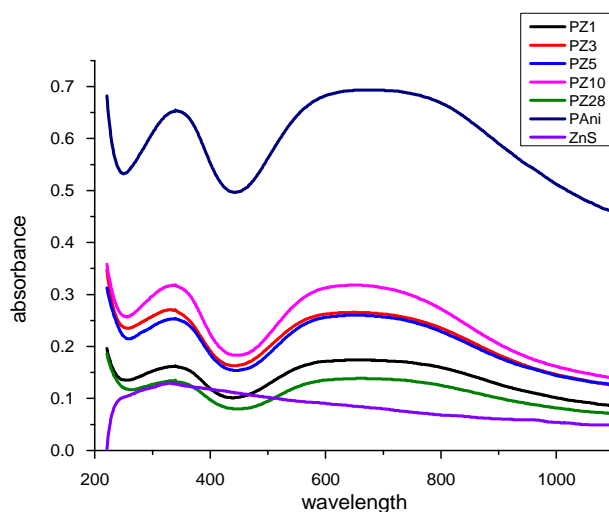


Figure 3: UV-Vis absorption spectra of nanocomposites

Pure PANi shows absorption peak at 340 nm and a broad band at 600 nm-800 nm. On forming composites with ZnS the 600-800 bands are shifted to the lower wavelength side with increasing concentration of ZnS. This indicates that ZnS nanoparticles have an effect on the absorption of PANi and it owes to an interaction at the interface of PANi and nano ZnS. Peak at 340 nm is due to Π - Π^* transition in the benzoid ring and peak at 620 nm is attributed to benzoid to quinoid excitonic transition in PANi [25]. The shape of UV-Vis spectra of PANi/ ZnS nanocomposite is similar to that of pure PANi. However a decrease at polaron band absorption implies that doping state of the nanocomposites has been improved. This can be attributed to greater number of charges on the polymer backbone by introducing nanocrystalline ZnS into polymer matrix. As a result the compacted coil structure would transform to an expanded coil structure [26].

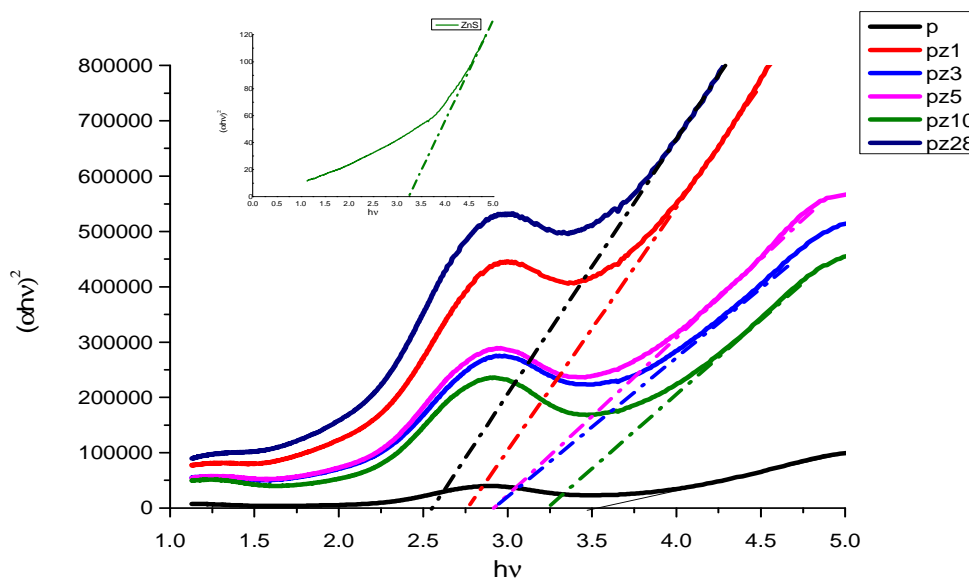


Figure 4: Determination of band gap energy for PANi and PANi/ZnSnanocomposite with various concentrations of ZnS

The observed band gaps for PANi, ZnS, PZ1, PZ3, PZ5, PZ10 and PZ 28 are 3.7, 5.0, 3.0, 2.9, 2.9, 3.2 and 2.5 respectively. It is found that optical band gap of composites decreases compared to bulk ZnS and PANi as shown in figure 4.

Photoluminescence

For measuring the photoluminescence the samples were excited at 320 nm wavelength radiations. Photoluminescence spectrum of PANi, ZnS and PANi/ZnS are shown in figure 5.

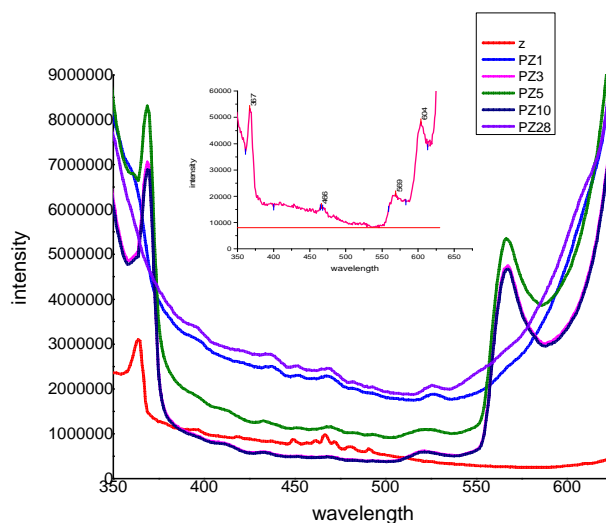


Figure 5: Photoluminescence spectrum of ZnS and PANi/ ZnS composites with PANi in inset

A broad PL emission peaked at 465 nm is obtained from donor-acceptor pairs in undoped ZnS [27]. The 365 nm emission is due to recombination of electrons at the sulphur vacancy donor level with holes trapped at the zinc acceptor level [28]. Peak at ~520 nm with less intensity could be due to some self activated defect centres related to Zn vacancies, reported in wurtzite ZnS [20]. In pure PANi there is a very low intensity photoluminescence peak observed at 567 nm. This is found to be enhanced in the nanocomposites. The intensity of this greenish yellow emission increases with increasing concentration of ZnS up to 10wt%, and is found to be completely quenched on addition of 28 wt% of ZnS in PANi. There are electron donating groups such as =NH in PANi and the electron withdrawing groups such as C=O of EDTA. This combination enhances the electron mobility in the composites and in turn favours the formation of singlet excitons. The singlet exciton states so formed decay radiatively to the ground state resulting in enhanced photoluminescence [17, 29], that is excitons are dissociated at the polymer/ nanocrystal interface, leaving the electron on the nanocrystal and hole on the polymer. A large fraction of excitons produced are dissociated at the interface, at low nanocrystal concentrations. Higher concentration of nanocrystal leads to the formation of separated electron - hole pairs that subsequently recombine nonradiatively at the interface leading to quenching. At higher concentration aggregation of the nanocrystals occurs and since the exciton diffusion ranges in conjugated polymers are in the 5-15 nm, any exciton which reaches a polymer/nanocrystal interface will be quenched [9]. Quenching is complete at higher concentration since the nanocrystals are randomly dispersed throughout the sample. Quenching in PANi/ ZnS nanocomposites indicates that charge transfer occurs at the polymer/nanocrystal interface.

Differential Scanning Calorimetry

Figure 6 shows DSC thermogram of the samples. All the samples exhibit a broad endothermic peak below 125°C, which is related to the release of moisture and other small molecules [22]. The endothermic peak around ~260°C is due to micro structural changes, that is cross linking and reorientation of PANi chain [18]. Structural decomposition and/or partial degradation of the PANi and nanocomposites occur at temperatures above 300°C [30]. The position of all the peaks in the nano composites shifts to the higher temperature with the increase in the ZnS concentration indicating the thermal stability and strengthening of the bonds. Shift of peak in the composites compared to PANi shows the interaction between ZnS nanoparticle and polyaniline matrix.

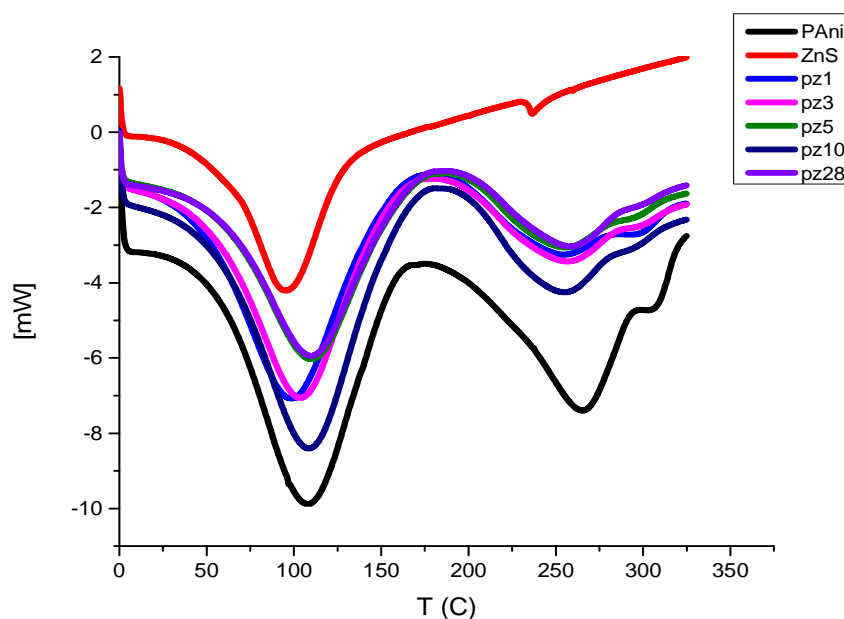


Figure 6: DSC of PANi, ZnS and Nanocomposites

DC conductivity

The temperature dependence of D.C. conductivity for PANi/ ZnS nanocomposites are studied with two probe set up and is shown in figure 7.

It is observed that conductivity is found to increase with increase in temperature. This increase in conductivity with temperature is the characteristic of "thermal activated behaviour". The increase in conductivity could be due to increase of efficiency of charge transfer between the polymer chains and the dopant with increase in temperature [26]. It is also possible that the thermal curing affects the chain alignment of polymer, which leads to the increase of

conjugation length and that brings about increase in conductivity. The conductivity of the composites is found to increase with increase in concentration of ZnS. At higher concentration (PZ28), conductivity of PANi/ ZnS nanocomposite is greater than that of pure PANi [31, 32].

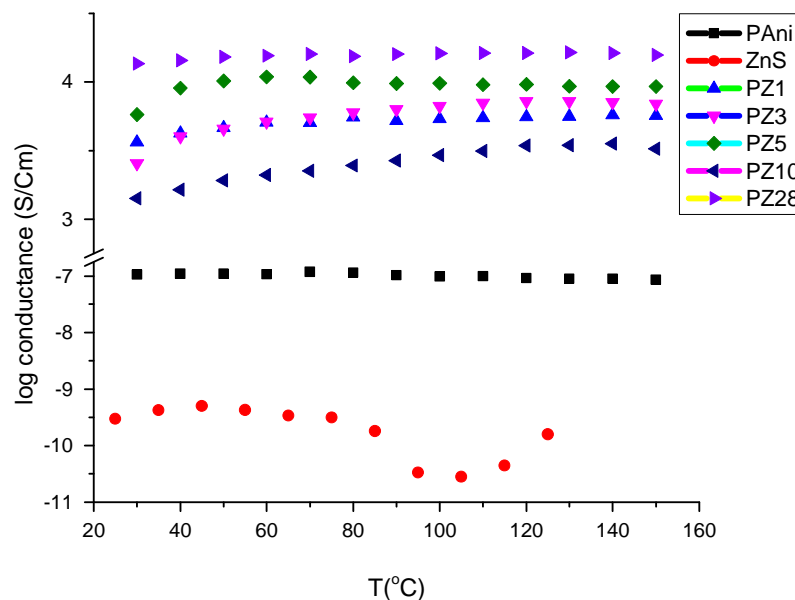


Figure 7: Log conductivity Vs Temperature graph of PANi, ZnS & PZ nanocomposites

Due to introduction of ZnS, electronic density of states increases in the polaronic band between the $\pi-\pi^*$ HOMO-LUMO structure of PANi at the PANi/ZnS interface. This increases the conductivity by increasing carrier concentration and the mobility and hence renders the interchain charge transport more efficient [33]. The enhancement in PL emission intensity is complimented by the enhancement in DC electrical conductivity. The increased crystallinity of PANi in the composites also supports the increased conductivity [34].

CONCLUSION

Different concentrations of PANi/ ZnS polymer nanocomposites have been prepared and their structural, optical and electrical properties are studied. XRD study shows that ZnS has wurtzite hexagonal structure in PANi /ZnS nanocomposites and the crystallinity of PANi increases with increase in content of ZnS in the composites. FESEM image shows the uniform dispersion in PANi. UV-Vis spectra show no additional peaks in the composites. An intense greenish yellow emission is obtained from PL spectra, whose intensity initially increases with increase in concentration, and later it is completely quenched at higher concentrations of ZnS in PANi. DC conductivity is seen to be in the semiconducting region. It is also found that the dc conductivity increases with concentration of ZnS in the composites. These results complement photoluminescence results. Increase in photoluminescence and quenching indicates the charge separation and transport at the interface of PANi/ZnS nanocomposites. DSC results show the structural changes in the polymer on heating. All these results indicate the formation of a stable and photoluminescent nanocomposites using this method. The photoluminescence in the sample makes them an interesting candidate for the construction of polymer light emitting diodes.

REFERENCES

- [1] F Capezzuto; G Carotenuto; F Antolini; E Burrese; M Palomba; P Perlo. *Express Polymer Letter*, **2009**, 3, 219–225.
- [2] M Dixit; S Gupta; V Mathur; K S Rathore; K Sharma; N S Saxena. *Chalcogenide Letters*, **2009**, 6 (3), 131 – 136.
- [3] J Z Mbese and P A Ajibade. *Polymers*, **2014**, 6, 2332 – 2344.
- [4] V Mathur and K Sharma. *Advances in Nanoparticles*, **2013**, 2, 205 – 216.
- [5] Aga and Mu. *Nanowires Science and Technology*, **2010**, 402.
- [6] C Ingrosso; A M Panniello; R Comparelli; M L Curri; M Striccoli. *Materials*, **2010**, 3, 1316 – 1352.

- [7] CO Oriakhi. Nano Sandwiches, *Chem. Br*, **1998**, 34, 59 – 62.
- [8] OO Christopher; M Lerner. Nanocomposites and Intercalation Compound, Encyclopaedia of Physical Science and Technology, (Reproduced in part with permission from Elsevier _ **2006**), **2001**, Vol. 10, 3rd ed.
- [9] NCGreenham; XiaogangPeng; AP Alivisatos. *Phys. Rev. B*, **1996**, 54, 17628-17637.
- [10] Reza Ansari and MB Keivani. *E-Journals of Chemistry*, **2006**, 3(4), 202 – 217.
- [11] A G MacDiarmid. *Angew chem. Int Ed Engl*, **2001**, 40(14), 2581 – 2590.
- [12] YT Ravikiran; MT Lagare; M Sairam; NNMallikarjuna; B Sreedhar; S Manohar; AG MacDiarmid; TM Aminabhavi. *Synthetic Metals*, **2006**, 156, 1139-1147.
- [13] K Dutta; S Manna; SK De. *Synthetic Metals*, **2009**, 159, 315 – 319
- [14] W Chen; ZWang; Z Lin; L Lin. *Journal of Applied Physics*, **1997**, 82(6), 3111 – 3115.
- [15] M Kanemoto; H Hosokawa; Y Wada, K Murakoshi; S Yanagida; T Sakata; H Mori; M Ishikawa; H Kobayashi. Journal of the Chemical Society, *Faraday Transaction*, **1996**, 92, 2401-2411.
- [16] M Sharma; D Kaushik; RR Singh; RK Pandey. *Journal of Material science: Materials in Electronics*, **2006**, 17(7), 537 – 541.
- [17] M Amrithesh; S Aravind; S Jayalekshmi; RS Jayasree. *Journals of Alloys and compounds*, **2008**, 449, 176 – 179.
- [18] A Singh; NP Singh; P Singh; R A Singh. *Journal of Polymer research*, **2011**, 18 (1), 67 – 77.
- [19] S Biswas; S Kar, *Nanotechnology*, **2008**, 19, 1-11.
- [20] B.SRemadevi; R. Raveendran; A.V. Vaidyan. *Pramana – Journal of Physics*, **2007**, 68(4), 679 – 687.
- [21] J B Bhaiswar; MY Salunkhe; S PDongre. *International Journals of Scientific and Research Publications*, **2013**, 3(1), 1 – 4.
- [22] M Amrithesh; S Aravind; S Jayalekshmi; RS Jayasree. *Journals of Alloys and compounds*, **2008**, 458, 532 – 535.
- [23] J Zhu; S Wei; L Zhang; Y Mao; JRyu; Neel Haldolaarachchige; David P.Young; ZGuo. *Journal of Materials chemistry*, **2011**, 21, 3952 – 3959.
- [24] X Lu; Y Yu; L Chen; H Mao; W Zhang; Y Wei. *Chemical Communications*, **2004**, 13, 1522 – 1523.
- [25] F.A. Mir. *Journal of Optoelectronics and Biomedical Materials*, **2010**, 2(2), 79- 84.
- [26] PS Khiew; NM Huang;S Radiman; Ahmed Md. Soot. *Material Letters*, **2004**, 58, 516 – 521.
- [27] S Sapara; A Prakash; A Ghangrekar; N Periasamy; DDSarma. *Journal of Physical Chemistry B*, **2005**, 109 (5), 1663- 1668.
- [28] W. Chen; V.F. Aguekian; N. Vassiliev; A. Yu Serov; N.G. Filosofov. *Journal of Chemical Physics*, **2005**, 123, 124707.
- [29] AKobyashi; H Ishikawa; K Amano; M Satoh. *Journal of Applied Physics*, **1993**, 74, 296.
- [30] AG MacDiarmid. *Current Applied Physics*, **2001**, 1, 269 – 279.
- [31] S M Reda and S M Al Ghannam. *Advances in Materials Physics and Chemistry*, **2012**, 2 (2), 75-81.
- [32] S Sarmah and A Kumar. *Bulletin of Material Science*, **2013**, 36, 31 – 36
- [33] H C Pant; M K Patra; S C Negi; A Bhatia; S R Vadera; N Kumar. *Bulletin of Material Science*, **2006**, 29 (4), 379 – 384.
- [34] A Lodha; S M KilbeyII; P C Ramamurthy; R V Gregory. *Journal of Applied Polymer Science*, **2001**, 82, 3602 – 3610.